

## Multi-Objective and Multi-Parameter Optimization of Solar Domestic Hot-Water Systems for Reducing On-Peak Power Consumption

Allan R. Starke<sup>1</sup>, Theo D. M. Ruas<sup>1</sup>, Samuel L. Abreu<sup>2</sup>, Jose M. Cardemil<sup>3,4</sup> and Sergio Colle<sup>1</sup>

<sup>1</sup> LEPTEN - Laboratory of Energy Conversion Engineering and Energy Technology/Federal University of Santa Catarina (UFSC), Florianópolis, Brazil.

<sup>2</sup> Federal Institute of Santa Catarina (IFSC), São José, Brazil

<sup>3</sup> School of Industrial Engineering, Universidad Diego Portales, Santiago, Chile

<sup>4</sup> Fraunhofer Chile Research Foundation, Center for Solar Energy Technologies. Santiago, Chile

### Abstract

Solar Domestic Hot-Water Systems can be a useful tool to reduce the energy consumption and on-peak power demand. This is particularly important in the case of Brazil where water heating in most cases is done using electrical showerheads with high installed power and low load factor. Consumers and utility companies have conflicting interests: reducing the electricity bill and shave the on-peak consumption. In the present work, these two interests were weighted and put together in the same objective function in order to find the trade-off curve with the optimized design parameters (collector area, storage volume and set point temperature) of the solar system. The analysis is carry out by considering two different policies: rebate program and time-of-use tariff (TOU). The results of the first policy show the existence of a trade-off curve between the initial investment and the yearly electricity consumption, which can be used to size the monetary incentive used for rebating the initial cost of the SDHW system. On the other hand, the results of the second policy shows a trade-off curve between the annualized life cycle cost of the system and the yearly on-peak electricity consumption, which can be used to size the TOU tariff as a function of the commitment of the utility company on reducing the on-peak electricity consumption.

Keywords: *Solar domestic hot-water systems, On-peak power consumption, Trade-off, Thermosyphon, Forced-circulation, TRNSYS.*

---

### 1. Introduction

Brazil owns one of the largest hydropower potential in the world (IEA, 2012a, 2010), because of that it currently represents the largest share on country's electricity matrix. In fact, electricity from renewable sources currently holds a share of about 80% (70.6% hydropower, 7.6% Biomass and 1.1% wind) (EPE, 2014). This scenario of strong dependence of the hydropower makes the grid very sensitive to the seasonal rain cycles. Long periods of drought have depleted water reservoirs in 2013 and 2014, reducing the security of the system and increasing the electricity costs.

In addition, 73% of the dwellings use electric showerheads for bathing (EPE, 2012). Because of the high consumption rate, this device represents about 24% of the residential electricity consumption. As a result, roughly 5.5% (33.7 TWh/year including losses) of the electricity consumption is due to the electric showerheads (ELETROBRAS, 2007). Averaging this value on a daily basis, a daily electricity consumption of about 92.4 GWh/day is accounted. Setting this result to the statistical load profile of the residential sector (ELETROBRAS, 2007), a power load curve for this device can be estimated, as shown in Figure 1a. As depicted by this figure, electric showerheads are indicated as responsible for the two peaks on the residential electric demand profile, between 5-9 AM and 5-9 PM, with values around 11 and 14 GW, respectively. It is

worth noting that on-peak consumption to supply the electric showerheads use in Brazil is an amount equivalent to the installed capacity of Itaipu, the second largest power plant in the world. Therefore, the electricity grid must be designed for supplying this peak, implying in high transmission and distribution costs for the system operator and utility companies.

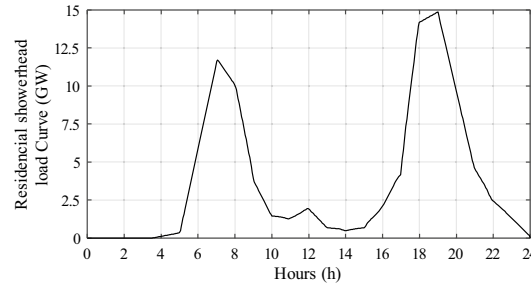


Fig. 1: Estimated showerhead load curve for Brazil.

The solar heating and cooling technologies can have an important role to play in realizing targets in energy security and economic development, especially the solar domestic hot water system, which is the most mature technology being used in a large scale since the 1960s (IEA, 2012b). This is not different for Brazil, the large-scale deployment of solar hot water system, could not only reduce the energy consumption that electric showerheads represents, but also reduce around 35 % of the on-peak power demand over the grid.

Currently, Brazil is the sixth country in total installed capacity of solar thermal collectors (IEA, 2012b). In fact, the energy supplied by solar thermal collectors currently operating in Brazil is around 4.3 GW<sub>th</sub> per year, which accounts for only 3.6% of the dwellings in Brazil (EPE, 2012). As observed in other countries, a strong increase in the deployment of solar hot water heating could be achieved by introducing long-term subsidy schemes or solar obligations. According to (IEA, 2011), Brazil has a solar thermal target of 15 million m<sup>2</sup> installed in 2015, from about 7 million m<sup>2</sup> in 2011, however financial support and public policies are restricted or inexistent. In this context, this paper assesses the feasibility of thermosyphon and forced-circulation solar domestic hot-water systems (SDHWs) submitted to two different policies: a rebate program and time-based tariff. For each policy, the systems are designed in terms of the solar collector area, the thermal storage volume and the set point temperature for the in-tank heater

The main goal of these policies is to promote the use of SDHWS, considering the interest of both, consumer and energy supplier. Therefore, the system needs to be cost-effective in the point of view of the consumer (i.e. reduce the energy consumption) and for the system operator and utility companies (i.e. reduce the peak consumption).

The first policy consists of a rebate program, aiming to assist low-income consumers to acquire proper SDHWs by means of rebating or partial financing the initial cost. This will be led by the electric utilities, since they have interest in reducing on-peak consumption (Borges et al., 2005). Therefore, this case presents the optimization regarding the on-peak consumption and the acquisition cost of SDHW. This yields a Pareto frontier that is used as a tool for sizing financial incentives to acquire a solar energy system (Liu et al., 2010).

In the second policy, a time-of-use tariff for the electricity is established to discourage the consumption on-peak hours (Borges et al., 2004; Borges, 2000). Thus, the on-peak consumption and Annualized Life Cycle Costs (ALCC) are optimized to find the trade-off between paying for the electricity at on-peak hours and the increase in the ALCC due a large investing in a SDHWs. In addition, an ideal value for the time-of-use tariff can be established based on how much the distributor is committed on reducing the peak consumption (Salazar, 2004).

The proposed methods are assessed through a multi-objective optimization that considers the relevant figures in both cases, which are evaluated by a long-term transient simulation routine. A case study is presented, regarding thermosyphon and forced-circulation SDHWs for Florianopolis – Brazil, considering the two policies under different scenarios. Moreover, two levels of daily hot water consumptions were considered, 0.2 and 0.4 m<sup>3</sup> at 40 °C, in order to analyze the sensitivity of the results for different hot-water demands.

## 2. System description

Two types of SDHWs are considered: thermosyphon and active (forced-circulation), as depicted in Figure 2. Thermosyphon systems, which work by natural circulation, are common in warm climates due the low probability of freezing, operational reliability and lower costs. This system avoids the use of pumps and dedicated control systems, however, the thermal storage needs to be placed at a higher position than the collector, and therefore is common to place it on the roof, limiting its size because of its weight and piping pressure drops.

Forced-circulation systems on the other hand, use a pump to circulate the water from the storage through the collector, allowing more flexibility on the installation of thermal storage, e.g it could be installed inside the house. Nevertheless, these systems are more complex, since they require a water pump and a differential temperature controller to ensure the proper operation of the system.

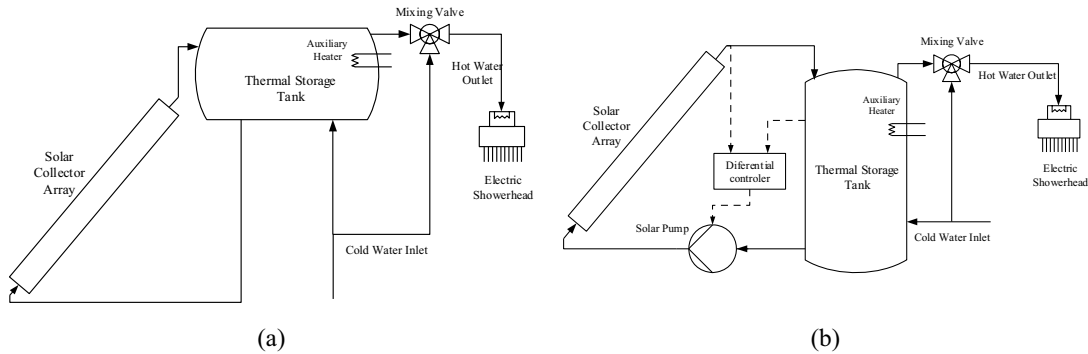


Fig. 2: Schematic diagram of the solar domestic hot water; (a) thermosyphon, and (b) forced-circulation.

The solar collector and thermal storage tank considered are identical for both systems, which specifications are presented in Table 1. The specifications of the solar collector were taken from (INMETRO, 2015), considering a class A solar collector randomly chosen. Meanwhile, the configuration of the thermosyphon system are shown in Table 2, and the main features of the forced-circulation system are shown in Table 3. It is worth to mention that in both systems water is used as heat transfer fluid and no heat exchanger is considered.

Tab. 1: Specification common to both system considered.

Parameter	Values
Collector slope, $\beta$ , ( $^{\circ}$ )	37.6
Intercept efficiency, $a_0$ , (-)	0.728
Efficiency slope, $a_1$ , ( $W/m^2K$ )	6.18
Incidence angle modifier coefficient, $b_0$ , (-)	0.1065
Tested flow rate, $F_{test}$ , ( $kg/m^2h$ )	60
Thermal storage shape factor, $S$ , (-)	0.5
Thermal storage insulation thickness, $e_i$ , ( $m$ )	0.05
Thermal storage insulation conductivity, $k_i$ , ( $W/mK$ )	0.126
Thermal storage maximum auxiliary heating rate, $P_{tank}$ , ( $kW$ )	3
Thermal storage auxiliary heating device efficiency, $\eta_{tank}$ , (-)	1
Thermal storage thermostat temperature dead band, $T_{db}$ , ( $^{\circ}C$ )	2
Electric showerhead maximum power, $P_{aux}$ , ( $kW$ )	10
Electric showerhead overall loss coefficient, $U_{aux}$ , ( $kJ/hK$ )	0
Electric showerhead efficiency, $\eta_{aux}$ , (-)	0.95
Electric showerhead set point, $T_{ideal}$ , ( $^{\circ}C$ )	40

Tab. 2: Specification of the thermosyphon system considered.

Parameter	Values
Riser diameter, $R_d$ , (m)	0.0142
Header diameter, $H_d$ , (m)	0.027
Collector inlet diameter, $d_i$ , (m)	0.015
Number of bends in the inlet pipeline, $Nb_1$ , (-)	4
Inlet pipeline thermal loss coefficient, $U_i$ , ( $kJ/m^2hK$ )	1.8
Collector outlet diameter, $d_o$ , (m)	0.019
Number of bends in the outlet pipeline, $Nb_2$ , (-)	4
Outlet pipeline thermal loss coefficient, $U_o$ , ( $kJ/m^2hK$ )	1.8
Height of the solar collector, $L_{col}$ , (m)	1.415
Vertical distance between collector's inlet and outlet, $H_c$ , (m)	0.864
Vertical distance between collector inlet and thermal storage outlet, $H_o$ , (m)	1.164
Thermal conductivity of the thermal storage and fluid entirety, $k_w$ , ( $W/mK$ )	2.207

**Tab. 3: Specification of the forced-circulation system considered.**

Parameter	Value
Ration between utilized and test flow rate, $R_{ca}$ , [-]	0.5
Upper temperature difference to trigger the solar pump, $T_{on}$ , ( $^{\circ}C$ )	6
Lower temperature difference to trigger the solar pump, $T_{off}$ , ( $^{\circ}C$ )	0.4

Some of the simulation parameters used in the systems are function of the design parameters (i.e. solar collector area and thermal storage volume), and need to be calculated in each iteration of the optimization process. These parameters are, thermal storage overall heat loss coefficient, thermal storage diameter and height, positions of the thermal storage thermostat and heating element, length of the solar collector and inlet piping length, number of parallel solar collector risers and maximum flow rate for the solar pump. The equations used to calculate these parameters were described in detail by Borges, (2000); Salazar, (2004)

It is worth noting that two auxiliary energy heaters were considered for both system, one inside the thermal storage and other in line to the load. The second one works as an electric showerhead and was considered in the simulation model just to ensure a comfortable water temperature for the users, in the case of the solar energy and the auxiliary heater of the tank were not able to supply the load.

The thermal performance of the SDHWs depends significantly on the domestic hot water load profile. In addition, it is impractical consider the daily and consumer variation, thus the suitable solution is to use a repetitive load profile (Kalogirou and Tripanagnostopoulos, 2006). In this paper, a statistically representative load profile was used, as depicted in Figure 3 in terms of a normalized figure. This profile was experimentally determined in a previous study (Salazar, 2004), where a group of ninety families were studied, by monitoring their electrical consumption of showerheads in one year period.

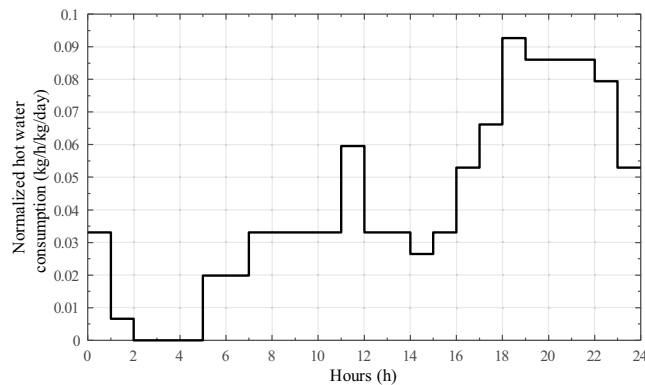


Fig. 3: Hot water daily consumption profile.

### 3. Methodology

The annual thermal performance and economic assessment, of both systems types, are determined by a transient simulation model. For that purpose, the Transient System Simulation Program (TRNSYS) (Klein, 2010) was used. Predicting the performance of solar systems by using simulation methods requires weather data input from the location where the system was installed. Therefore, the TMY file available from SWERA database (SWERA, 2013) for Florianopolis (27.6°S/48.5°W) was employed in this study.

The performance of the thermosyphon system was calculated through the (Morrison and Braun, 1985) model, whereas the one-tank forced-circulation system was considered as a stratified thermal storage with fixed inlet (Cooper et al., 1975). In addition, the auxiliary energy supply were simulated as electric heaters with a fixed thermal efficiency and with a maximum power (Table 1). Therefore, the actual power is modulated to meet the specified set point temperature.

Each system needs to be proper sized when submitted to two different policies that can be expressed as objective functions. Thus, an optimization routine was applied to the systems considering three design parameters as independent variables: the solar collector area, the thermal storage volume and the set point temperature for the in-tank heater. The combination of an optimization routine with a life-cycle simulation of a solar system was extensively explained by Borges et al., (2005).

Since the two used policies consider conflicting objectives between the consumer and the energy supplier, a weighted global criterion method was employed to accurately represent the behavior of these objectives in the optimization problems. With the weighted global criterion method, it is possible to solve a single objective by assigning relative weights ( $\varphi$ ) to the conflicting ones (Borges et al., 2004, 2005; Marler and Arora, 2004)

The Generic Optimization Program (GENOPT) was used for the multi-objective and multi-parameter optimization, since it can be easily coupled with TRNSYS. This software has a large optimization algorithm library from which the hybrid algorithm of the Particle Swarm Optimization algorithm and the Generalized Pattern Search implementation of the Hooke-Jeeves algorithm (GPSPSOCCHJ) were selected. This decision is adequate for specific features of problems in which the objective function is not continuously differentiable, or it must be approximated, which is the case of the thermal simulation routines analyzed. Therefore, the design parameters can be only solved heuristically (Wetter, 2008).

#### 3.1. Rebate program

The rebate program considers that the two conflicting objectives are the on-peak yearly energy consumption ( $E_{peak}$ ) and the initial investment of the solar system ( $IC$ ), where the on-peak period is from 5 to 9 PM. Therefore, the optimization problem can be defined as follows,

$$\min_{\vec{x}} \left\{ f(\vec{x}) = (1 - \varphi) \frac{E_{peak}(\vec{x})}{E_{peak,max}} + \varphi \frac{IC(\vec{x})}{IC_{max}} + C_1 P_1(\vec{x}) + C_2 P_2(\vec{x}) \right\}$$

Subject to:

$$\vec{x} \in S$$

$$P_1(\vec{x}) = \begin{cases} 0, & \text{if } ALCC \leq ALCC_{limit} \\ (ALCC_{limit} - ALCC(\vec{x}))^2, & \text{otherwise} \end{cases} \quad (\text{eq. 1})$$

$$P_2(\vec{x}) = \sum_t \begin{cases} 1, & \text{if } T_{cons}(\vec{x}) < T_{ideal} \\ 0, & \text{otherwise} \end{cases}$$

where  $S$  is the feasible region defined by the solar collector area ( $A_c$ ), thermal storage volume ( $V_{tes}$ ) and set point temperature for the in-tank heater.  $E_{peak,max}$  and  $IC_{max}$  are the maximum values of the on-peak yearly energy consumption and initial cost possible on the feasible region, which were used to rewrite the two

conflicting objectives in a non-dimensional form. To do so, the optimization software was employed to find the maximum feasible values for each of the objectives, before the objective function were implemented in the simulation environment.

Two constrains were considered in this optimization problems, the first is used to guarantee that the annualize life cycle cost of the system ( $ALCC$ ) will be less than a specified value ( $ALCC_{limit}$ ), and the second is used to guarantee that the system supplies water at the desired temperature ( $T_{ideal}$ ). This constrained optimization problem was solved using a penalty method. (i.e. a constant value is added in the objective function when the constrained event is triggered), which are the two last terms on the right of the equation 1 ( $C_1P_1(\vec{x})$  and  $C_2P_2(\vec{x})$ ).

Since the relative importance of each conflicting function is not known, the domain of  $\varphi$  is divided in a series of discreet values and single objective optimizations were run for each value of  $\varphi$ . The results of this analysis can be presented by a curve (Pareto frontier) representing the initial cost versus on-peak yearly energy consumption. This curve is used as a tool for sizing financial incentives to acquire a system, as a solution for decreasing the on-peak power consumption. The methodology and the economic assumptions used for calculating the  $ALCC$  and  $IC$  are described in the section 3.3.

### 3.2. Time-of-use tariff

For this policy, the two conflicting objectives considered are the on-peak yearly energy consumption and  $ALCC$  of the system. The period between 5 and 9 PM was considered as on-peak for applying the higher electricity tariff. In addition, the constraint used to guarantee that the system supply water is in the desired temperature to the consumers ( $T_{ideal}$ ) is also considered. Therefore, the optimization problem can be defined as follows,

$$\min_{\vec{x}} \left\{ f(\vec{x}) = (1 - \varphi) \frac{E_{peak}(\vec{x})}{E_{peak,max}} + \varphi \frac{ALCC_0(\vec{x})}{ALCC_{0,max}} + C_2P_2(\vec{x}) \right\}$$

Subject to:

$$\vec{x} \in S$$

(eq. 2)

$$P_2(\vec{x}) = \sum_t \begin{cases} 1, & \text{if } T_{cons}(\vec{x}) < T_{ideal} \\ 0, & \text{otherwise} \end{cases}$$

where  $ALCC_0$  is the annualized life cycle cost considering only the nominal value of the electricity tariff ( $C_e$ ) and  $ALCC_{0,max}$  is the maximum annualized life cycle cost possible on the feasible region. The equation 2 considers only the nominal tariff, in order to minimize the number of optimization runs. Different values of the tariff were considered in a post-processing procedure, in which the following equation was used,

$$ALCC(\vec{x}) = ALCC_0(\vec{x}) + E_{peak}(\vec{x})C_{e,TOU} \quad (\text{eq. 3})$$

where  $ALCC$  is the total annualized life cycle cost, considering the time-of-use tariff -  $C_{e,TOU}$ , defined as the surcharge value added to the nominal electric tariff ( $C_e$ ) during the on-peak hours. This approach removes the need of run the optimization routine for each time-of-use tariff. It is worth mention that in the case of a null value for the time-of-use tariff, the expression is reduced to  $ALCC(\vec{x}) = ALCC_0(\vec{x})$ .

Hence, the results of this analysis can be presented by a curve of  $ALCC$  versus  $E_{peak}$ , for different values of the time-of-use tariff, showing the trade-off between paying for the electricity at on-peak hours and the increase in the  $ALCC$  due a large investment on a SDHW.

### 3.3. Economic Figures

In order to determine the economic figures derived from the optimization processes, the life-cycle cost analysis

was considered according to (Duffie and Beckman, 2013),

$$LCC(\vec{x}) = (1 + C_{inst})IC(\vec{x})[1 + C_m PWF(N, i_m, d)] + PWF(N, 0, d)E_{aux}(\vec{x})C_e \quad (\text{eq. 4})$$

where  $C_{inst}$  is the installation cost as a percentage of the initial cost,  $C_m$  is the annual maintenance cost as a percentage of the installed cost of the system,  $E_{aux}$  is the total auxiliary yearly energy consumption,  $PWF$  is the present-worth factor,  $N$  is the lifetime of the system,  $i_m$  is the maintenance inflation rate and  $d$  is the discount rate. In order to analyze the system on a yearly basis, the life-cycle cost can be annualized by the following equation,

$$ALCC(\vec{x}) = \frac{LCC(\vec{x})}{PWF(N, 0, d)} \quad (\text{eq. 5})$$

Finally, the initial cost can be calculated as follows,

$$IC(\vec{x}) = (C_c A_c + C_{tes}(V_{tes}) + C_a P_{tank}) \quad (\text{eq. 6})$$

where  $C_c$  is the solar collector cost per area,  $A_c$  is the solar collector area,  $C_{tes}$  is the thermal storage cost as a function of the storage tank volume ( $V_{tes}$ ),  $C_a$  is the cost of the heating element per power and  $P_{tank}$  is the electric power of the auxiliary heater in the thermal storage.

The economic parameters considered herein are representative of the Brazilian market at the time of the study and listed in Table 4.

Tab. 4: Economic and cost considerations.

Parameter	Value
Solar system life cycle, $N$ , (years)	20
Discount rate, $d$ (%)	8
Maintenance inflation rate, $i_m$ (%)	6.4
Solar collector cost, $C_c$ (€/m <sup>2</sup> )	119.25
Heating element cost, $C_a$ (€/kW)	6.9
Annual maintenance cost, $C_m$ (% of installed cost)	1
Installation cost, $C_{inst}$ (% of initial cost)	15
Nominal value of the electric tariff, $C_e$ (€/kWh)	0.1385
Exchange rates for Euro at March, 2014, $u$ (BR\$/€)	3.48

The cost, in euros, of the thermal storage ( $C_{tes}$ ) was considered in the analysis by a regression model based on the prices of tanks with different volumes obtained of the main suppliers in the Brazilian market, as follows,

$$C_{tes}(V_{tes}) = \frac{1}{u}(4798.8V_{tes} - 2889.8V_{tes}^2 + 1196V_{tes}^3 - 216.9V_{tes}^4 + 14.911V_{tes}^5) \quad (\text{eq. 7})$$

## 4. Results

The results of the case study are presented for Florianopolis – Brazil (27.6°S/48.5°W), considering the thermosyphon and forced-circulation SDHWs, where two levels of daily hot water consumptions were considered, 0.2 m<sup>3</sup> and 0.4 m<sup>3</sup>, both at 40 °C. These values were chosen because they can represent low-income consumers and standard consumers, respectively.

Regarding the rebate program, eight values of the  $ALCC_{limit}$  were considered 130, 185, 200 and 215 €/year for low-income scenario, and 260, 370, 400 and 430 €/year for the standard consumer scenario. On the other hand, four values of the time-of-use tariff were considered in the time-based program: 0, 0.5, 1 and 2 €/kWh. Where these values are added to the nominal value of the electricity tariff in the period between 5 and 9 PM.

### 4.1. Rebate program

The trade-off between initial cost and yearly on-peak electricity consumption for an  $ALCC_{limit}$  of 215 and 430

€/year, for the scenarios of 0.2 m<sup>3</sup> and 0.4 m<sup>3</sup> respectively, is depicted in Figure 4. Each point of these curves represent a result of the optimization process, with different design values that simultaneously minimize the weighted combination of the yearly on-peak electricity consumption and initial cost.

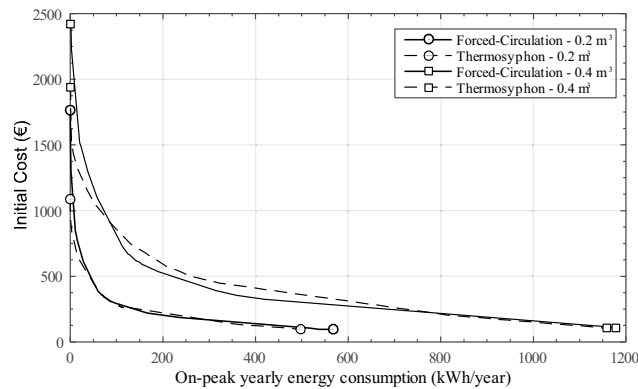


Fig. 4: Trade-off curves between initial cost and yearly on-peak electricity consumption obtained by the rebate program for an  $ALCC_{limit}$  of 215 and 430 €/year for the scenarios of 0.2 m<sup>3</sup> and 0.4 m<sup>3</sup>, respectively.

Three regions can be identified in figure 4, on the left, with high initial cost and low yearly on-peak electricity consumption there is the adverse region for the consumer, where a decrease in the on-peak electricity consumption represents a large increase on the initial cost. In contrast, on the right is observed the adverse region for the utility companies, characterized by low initial cost and high yearly on-peak electricity consumption, in this region a decrease on the initial cost represents a large increase on the on-peak electricity consumption. Finally, between these two regions, the negotiation region is observed, depicted by a small increase on the initial cost which represents a large reduction on the on-peak electricity consumption.

Within the negotiation region, systems with 0.2 m<sup>3</sup> of daily consumption, show an increase from 150 to 250 € on the initial cost, providing a reduction from 325 to 125 kWh/year on the yearly on-peak consumption. It means that rebating 40% on the initial cost (100 € of 250 €) will provide a reduction of 62 % in the on-peak consumption, a result highly interesting for the utility companies.

Regarding the systems with 0.4 m<sup>3</sup> of daily consumption, an increase from 300 to 400 € in the initial cost, gives a reduction between 500 to 300 kWh/year on the yearly on-peak electricity consumption. Meaning that rebating 25% on the initial cost (100 € of 400 €) will provide a reduction of 40 % on the on-peak consumption.

Finally, it is worth noting that for 0.2 m<sup>3</sup> of daily consumption of hot water, both thermosyphon and forced-circulation systems present similar results. Moreover, for 0.4 m<sup>3</sup>, the forced-circulation system present lower values of on-peak yearly electricity consumption for the same initial cost. That result indicates that the forced-circulation system could be more effective in reducing the on-peak consumption, however, these are minor differences.

Figure 5, shows the effect of the  $ALCC_{limit}$  in the trade-off curves for both the thermosyphon and forced-circulation systems, for the case of 0.2 m<sup>3</sup> of daily consumption. It can be noticed that the limitation on the  $ALCC$ , reduces the domain of solutions that met the objective function, therefore, reduces the size of the trade-off curves and the negotiation region.

The proposed methodology helps defining the monetary incentive used for rebating the initial cost of the SDHWs, however, the proper size of this incentive can be only defined by the utility company and with its commitment in reducing the on-peak consumption.



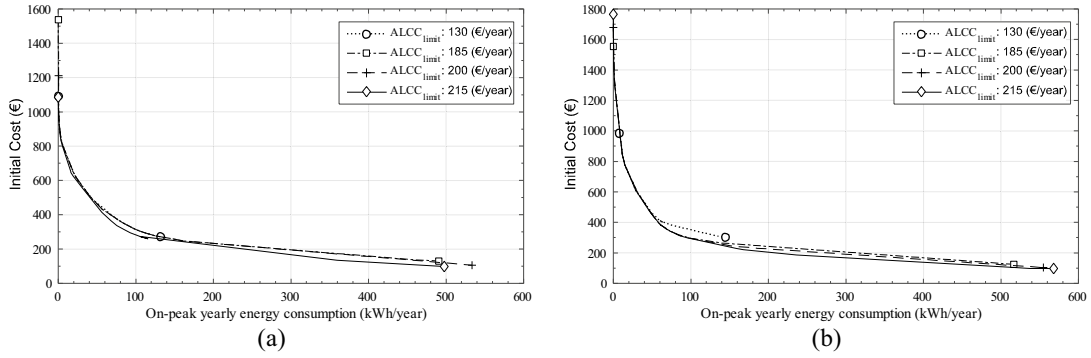


Fig. 5: Effect of the  $ALCC_{limit}$  in the trade-off curves of the rebate program for thermosyphon (a), and forced-circulation (b) systems for a  $0.2 \text{ m}^3$  of hot water consumption.

#### 4.2. Time-of-use tariff

The trade-off between the annualized life cycle cost of the system and the on-peak yearly electricity consumption are shown in Figure 6, where curves for the thermosyphon and forced-circulation are observed. The curves represented by a null value of time-of-use tariff (TOU tariff) were obtained by the optimization process using equation 2. On the other hand, the other curves were calculated as a post-processing procedure using equation 3, which allows consider different values for time-of-use tariff.

It can be seen that the results are very similar for  $0.2 \text{ m}^3$  and  $0.4 \text{ m}^3$  of hot water consumption, where the difference is due to a matter of scale. Moreover, under this policy the thermosyphon system shows better performance, being more effective on reducing the on-peak yearly electricity consumption.

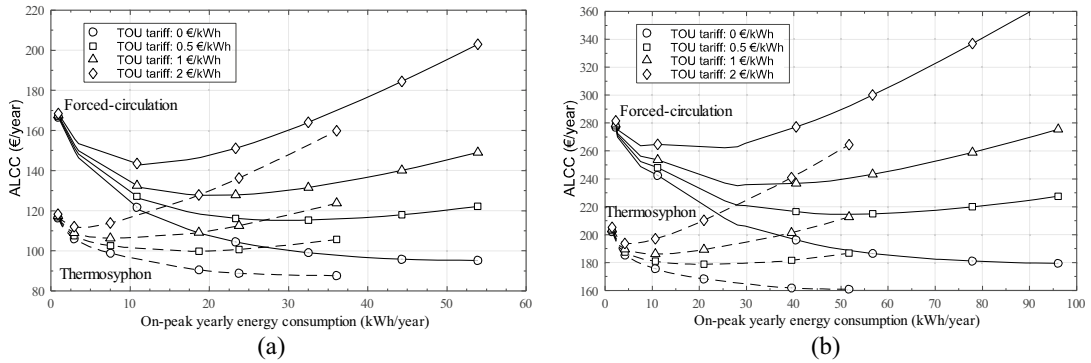


Fig. 6: The trade-off between the annualized life cycle cost of the system and the on-peak yearly electricity consumption for the thermosyphon and for-circulation system for  $0.2 \text{ m}^3$  (a), and  $0.4 \text{ m}^3$  (b) of hot water consumption.

Regarding the different values of the TOU tariff, it can be noted that for each tariff exists a minimal value of the ALCC, indicating the optimal design for the consumer. Therefore, each minimal ALCC and its respective on-peak yearly electricity consumption can be calculated for each value of the time-of-use tariff. This is achieved by deriving the equation 3 with respect of the yearly on-peak consumption and equating to zero (minimal ALCC), as follows,

$$\frac{dALCC(\vec{x})}{dE_{peak}} = \frac{dALCC_0(\vec{x})}{dE_{peak}} + C_{e,TOU} = 0 \quad (\text{eq. 8})$$

where the  $dALCC_0(\vec{x})/dE_{peak}$  can be calculated numerically or analytically if a regression model is applied in the  $ALCC_0$  versus  $E_{peak}$  curve. Rearranging the equation 8, the intended time-of-use tariff  $C_{e,TOU}^*$  can be calculated as follows,

$$C_{e,TOU}^* = -\frac{dALCC_0(\vec{x})}{dE_{peak}} \quad (\text{eq. 9})$$

This quantity can be plotted as a function of the on-peak yearly electricity consumption, as depicted in Figure

7. This methodology provides a tool for sizing the values of the time-of-use tariff in function of the commitment for reducing the on-peak consumption. Moreover, it is clear the existence of a negotiation region, where a small value for the TOU tariff can reduce in more than half the on-peak consumption.

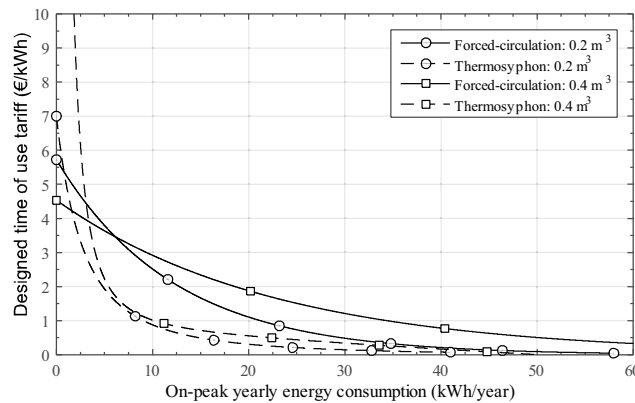


Fig. 7: Designed time-of-use tariff for the forced-circulation and thermosyphon system, considering both 0.2 m<sup>3</sup> and 0.4 m<sup>3</sup> of hot water consumption.

Figure 7 shows that the designed values of the TOU tariff are similar for the thermosyphon system, regardless the level of hot water consumption. However, this trend is not observed for the forced-circulation system. When the system faces higher consumption, a higher TOU tariff is required to archive the same degree of reduction on the on-peak electricity consumption.

## 5. Conclusions

This work presented two methodologies for sizing financial policies for SDHWs, and measure its effectiveness on the reduction of on-peak electricity consumption. The approach analyzed herein considered the interest of both, consumer and energy supplier.

The first policy, rebate program, uses a trade-off curve between initial cost and yearly on-peak electricity consumption, where a clear negotiation region is identified. Therefore, it could be used as a design tool for defining the monetary incentive used for rebating the initial cost of the SDHW system, as a function of the commitment on reducing the on-peak consumption by the utility company

The second policy, time-of-use tariff, uses a trade-off curve between the annualized life cycle cost of the system and the yearly on-peak electricity consumption, for different time-of-use tariffs. This procedure shows the existence of a minimal value of the ALCC for each TOU tariff, indicating the optimal design for the consumer. Consequently, it is possible to determine the value of the on-peak yearly electricity consumption respective to the minimal ALCC, for each TOU tariff adopted. This yields a trade-off curve between the designed time-of-use tariff and the on-peak yearly electricity consumption, which helps to size the TOU tariff as a function of the commitment of the utility company on reducing the on-peak electricity consumption.

## 6. References

Borges, T.P., Colle, S., Wendel, M., 2004. IMPACTOS DA ADOÇÃO DE TARIFAS DIFERENCIADAS DE ENERGIA ELÉTRICA SOBRE O PROJETO OTIMIZADO DE SISTEMAS DE AQUECIMENTO SOLAR DE ÁGUA, in: Vázquez, M., Seara, J.F. (Eds.), XII Congreso Ibérico Y VII Congreso Iberoamericano de Energía Solar. Vigo, España, pp. 14–18.

Borges, T.P.D.F., 2000. Síntese otimizada de sistemas de aquecimento solar de água. Universidade Estadual de Campinas.

Borges, T.P.F., Colle, S., Wendel, M., 2005. Multiobjective Optimization as a Decision Tool for Financing or Rebating Domestic Solar Water Heaters, in: Solar World Congress - ISES 2005. Orlando, USA, pp. 2–6.

Cooper, P.I., Klein, S.A., Dixon, C.W.S., 1975. Experimental and Simulated Performance of a Closed Loop

Solar Water Heating System, in: ISES 1975 International Solar Energy Congress.

Duffie, J.A., Beckman, W.A., 2013. *Solar Engineering of Thermal Processes*, Fourth Ed. ed. Wiley, New Jersey. doi:10.1002/9781118671603

ELETROBRAS, 2007. *Avaliação do Mercado de Eficiência Energética no Brasil. Pesquisa de Posse de Equipamentos e Hábitos de Uso (ano base 2005) - Classe Residencial – Relatório Brasil*. Rio de Janeiro.

EPE, 2014. *Brazilian Energy Balance 2014 - Year 2013*. Rio de Janeiro.

EPE, 2012. *NOTA TÉCNICA DEA 16/12 Avaliação da Eficiência Energética para os próximos 10 anos (2012-2021) - Série Estudos de Demanda*. Rio de Janeiro.

IEA, 2012a. *Technology Roadmap: Hydropower*. Springer-Verlag, Paris, France.

IEA, 2012b. *Technology Roadmap: Solar Heating and Cooling*. Paris, France.

IEA, 2011. *G-20 Clean Energy, and Energy Efficiency Deployment and Policy Progress*. Paris, France.

IEA, 2010. *Renewable Energy Essentials: Hydropower*. Paris, France.

INMETRO, 2015. *SISTEMAS E EQUIPAMENTOS PARA AQUECIMENTO SOLAR DE ÁGUA - COLETORES SOLARES*. Brasília - Brazil.

Kalogirou, S.A., Tripanagnostopoulos, Y., 2006. Hybrid PV/T solar systems for domestic hot water and electricity production. *Energy Convers. Manag.* 47, 3368–3382. doi:10.1016/j.enconman.2006.01.012

Klein, S.A., 2010. *TRNSYS: A transient systems simulation program*, V. 17.

Liu, P., Pistikopoulos, E.N., Li, Z., 2010. An energy systems engineering approach to the optimal design of energy systems in commercial buildings. *Energy Policy* 38, 4224–4231. doi:10.1016/j.enpol.2010.03.051

Marler, R.T., Arora, J.S., 2004. Survey of multi-objective optimization methods for engineering. *Struct. Multidiscip. Optim.* 26, 369–395. doi:10.1007/s00158-003-0368-6

Morrison, G.L., Braun, J.E., 1985. System modelling and operation characteristics of thermosyphon solar water heaters. *Sol. Energy* 34, 389–405. doi:10.1016/0038-092X(86)90024-1

Salazar, J.P. de L.C., 2004. *Economia de energia e redução do pico da curva de demanda para consumidores de baixa renda por agregação de energia solar térmica*. Universidade Federal de Santa Catarina.

SWERA, 2013. *Solar and Wind Energy Resource Assessment [WWW Document]*. URL <http://en.openei.org/wiki/SWERA/Data>

Wetter, M., 2008. *GenOpt - Generic Optimization Program - User Manual V 2.1.0*.